Polarization entanglement and quantum beats of photon pairs from four-wave mixing in a cold ^{87}Rb ensemble

Gurpreet Kaur Gulati

Center for Quantum Technologies, National University of Singapore,
3 Science Drive 2, Singapore, 117543

Bharath Srivathsan

Center for Quantum Technologies, National University of Singapore,
3 Science Drive 2, Singapore, 117543

Brenda Chng

Center for Quantum Technologies, National University of Singapore,
3 Science Drive 2, Singapore, 117543

Alessandro Cerè

Center for Quantum Technologies, National University of Singapore,
3 Science Drive 2, Singapore, 117543

Christian Kurtsiefer[1,2]

[1]Center for Quantum Technologies, National University of Singapore,
3 Science Drive 2, Singapore, 117543
[2]Department of Physics, National University of Singapore, 2 Science Drive 3,
Singapore, 117542

E-mail: `christian.kurtsiefer@gmail.com`

Abstract. We characterize correlations in polarization and time of photon pairs generated from a cold cloud of ^{87}Rb atoms via a four-wave mixing process in a cascade level scheme. Quantum state tomography reveals entangled polarization states of high purity for each of the decay paths through two different intermediate hyperfine levels. When allowing both decay paths, we observe quantum beats in time-resolved correlation measurements.

1. Introduction

Time-correlated and entangled photon pairs have been an important resource for a wide range of quantum optics experiments, ranging from fundamental tests [1] to applications in quantum communication, cryptography, teleportation and computation [2].

The first sources of correlated photon pairs were based on a cascade decay in neutral atoms [3, 4]. The cascade imposes a time correlation, and with an appropriate choice of the geometry and intermediate states it is possible to observe a strong non-classical correlation in the polarization of the photons. These sources are rarely used today in quantum optics experiments for their limited generation rates, and have been superseded by schemes based on three-wave mixing in non-linear optical crystals, or four-wave mixing (FWM) in optical fibers [5]. To obtain a narrow optical bandwidth, it is possible to use near-resonant transitions in atoms to provide the large third order nonlinear susceptibility for efficient FWM, leading to photon pairs with a central wavelength matching those of the transitions involved [6, 7, 8]. These sources are a hybrid between the traditional atomic cascade approaches, and those based on three- or four-wave mixing in solids in the sense that they deliver both a useful pair rate collected into single mode optical fibers, and exhibit interesting temporal correlations.

In this paper, we present the characterization of a source of time-correlated and polarization-entangled photon pairs based on four-wave mixing in a cold cloud of ^{87}Rb atoms. The involved atomic levels, selected by the choice of pump and target wavelengths, form a cascade decay scheme, providing an asymmetrical time correlation similar to the one from the cascade decay of single atoms.

2. Polarization entanglement

Entanglement between photons can be established in several degrees of freedom like time bins, polarization, and orbital angular momentum [9], with polarization entanglement having been extensively studied due to its robustness and the availability of very stable optical elements for manipulating and detecting the polarization of single photons [10].

Observation of photon polarization entanglement begin with early photon pair sources based on cascade decays in atomic beams [11], followed by spontaneous parametric down conversion in nonlinear optical crystals [12], cold [8] and hot [13] atomic vapors, and recently also in cascade emission from quantum dots [14]. In this paper, we characterize the correlation polarization properties of nearly Fourier-limited photon pairs generated from the cold cloud of ^{87}Rb [15, 16].

3. Experimental setup

The experimental setup is similar to our earlier work [15, 16], but uses a collinear beam geometry (see figure 1). An ensemble of cold ^{87}Rb atoms is prepared with a magneto-optical trap (MOT) of optical density OD $\approx$ 32 for light resonant to the $5S_{1/2}, F = 2$
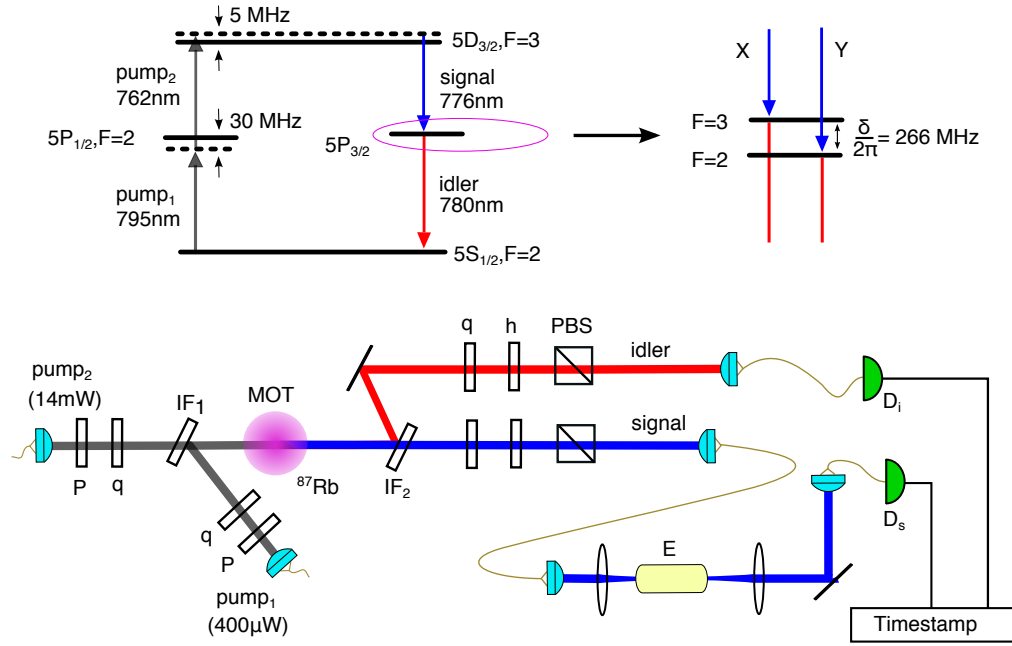
Figure 1.   Level scheme for four-wave mixing in ^{87}Rb, and schematic of the experiment. A first interference filter (IF$_1$) combines the two pump beams in a co-propagating geometry inside the cloud, a second one (IF$_2$) separates the signal and idler photons from residual pump light. The pump polarizations can be freely chosen with polarizers (P) and quarter wave plates (q). A stack of quarter wave plate, half wave plate (h), and polarizing beam splitter (PBS) in each collection mode can select any arbitrary polarization. A solid etalon (E) can be used to select light from only one for the decay paths X and Y. Di, Ds: Avalanche Photodetectors.

$\rightarrow 5\mathrm{P}_{3/2}$, $F = 3$ transition. The atoms are excited from $5\mathrm{S}_{1/2}, F = 2$ to $5\mathrm{D}_{3/2}, F = 3$ via a two-photon transition, with a two-photon detuning of $\approx 5\,\mathrm{MHz}$. Pump beams of wavelength $795\,\mathrm{nm}$ and $762\,\mathrm{nm}$ overlap in a co-propagating geometry inside the cloud. The $795\,\mathrm{nm}$ pump is red detuned by $30\,\mathrm{MHz}$ from the intermediate level $5\mathrm{P}_{1/2}$, $F = 2$ to reduce the incoherent scattering rate. From the $5\mathrm{D}_{3/2}$, $F = 3$ excited level, atoms can decay through several paths. We select "signal" photons around $776\,\mathrm{nm}$, and "idler" photons around $780\,\mathrm{nm}$ with interference filters of $3\,\mathrm{nm}$ FWHM bandwidth. Within this bandwidth, two decays can be observed (figure 1, top right): decay X through the hyperfine level $5\mathrm{P}_{3/2}$, $F = 3$, and Y going through $5\mathrm{P}_{3/2}$, $F = 2$.

Energy conservation and phase matching results in the generation of signal and idler photon pairs from both decay paths with a frequency difference of $\delta{=}266\,\mathrm{MHz}$ corresponding to the hyperfine splitting of the intermediate level. The generated photons are collected into single-mode fibers and detected by avalanche photodetectors (quantum efficiency $\approx 40\%$, jitter time $\approx 1\,\mathrm{ns}$). In the experiment, we cycle between a $150\,\mu\mathrm{s}$ long cooling period with the MOT turned on, and a $10\,\mu\mathrm{s}$ long period for pair generation.
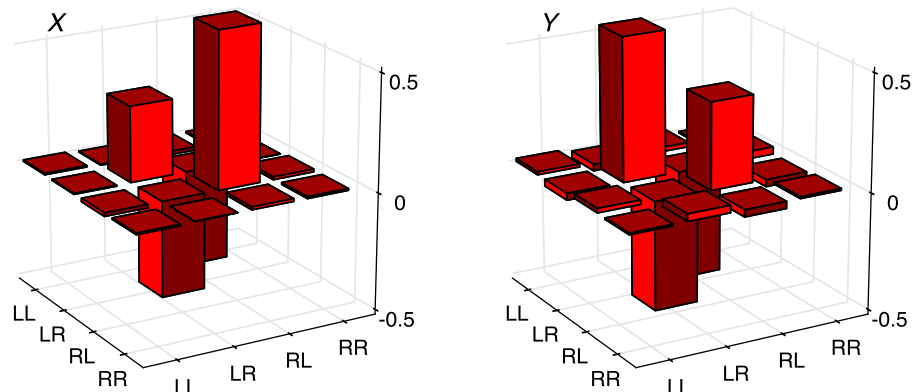
Figure 2. Tomographic reconstruction of the polarization state ρ (real part) for biphotons generated via decay path X (on the left), and Y (right), for pump modes set to orthogonal circular polarizations. The imaginary part of all matrix elements is below 0.09 and is not shown.

4. Polarization state tomography

We investigate the polarization state of the photon pairs for decay paths X and Y independently. We select light in the signal mode (see figure 1) using a 2 cm long solid fused silica etalon with a transmission bandwidth of 52 MHz (FWHM). The etalon is temperature-tuned to match to the resonance frequency of either the $5P_{3/2}, F = 3 \rightarrow 5D_{3/2}, F = 3$ or $5P_{3/2}, F = 2 \rightarrow 5D_{3/2}, F = 3$ transition; its temperature is stabilized to within 1 mK to minimize frequency drifts.

We completely characterize the polarization state of photon pairs via quantum state tomography [17] by projective detections of individual photons in a combination of linear and circular polarizations. For this, we insert quarter and half wave plates (q, h) followed by beam splitter cubes (PBS) in the signal and idler modes. Figure 2 shows the real part of the reconstructed biphoton states ρ_X and ρ_Y corresponding to decay paths X and Y. The imaginary parts of all elements are smaller than $\pm 0.09i$. The strong off-diagonal elements (LR, RL) signify the polarization entanglement. From the reconstructed matrices, we can extract typical entanglement measures for the state; we evaluate the concurrence C [18], and the entanglement of formation E [19]. Furthermore, we can also determine the purity $P = \text{Tr}[\rho_{X,Y}^2]$ of the biphoton state for each decay path. The values of these indicators are given in table 1.

Despite the fact that the atomic ensemble is not prepared in a particular Zeeman sublevel, the polarization states for photon pairs from both decay paths show a remarkably high purity. This is compatible with theoretical models presented in [20, 21], which we briefly summarize here.

In a cascade decay, polarization entanglement arises from indistinguishable decay

	X	Y
Purity P	0.92±0.02	0.96±0.03
Concurrence C	0.89±0.01	0.94±0.01
Entanglement of formation E	0.85±0.03	0.98±0.01

Table 1. Entanglement indicators for reconstructed states $\rho_{X,Y}$. The uncertainties reflect propagated Poissonian counting statistics of contributing coincidence events.

paths, in our case provided by sufficiently degenerate Zeeman states of each hyperfine level. With the quantization axis along the beam propagation direction of all modes, we only drive transitions with $\Delta m_F = \pm 1$ with orthogonally circularly polarized pump beams. In parametric processes [22], the quantum state of the medium remains unchanged through the interaction [23]. Further, rotational symmetry of the atomic cloud in beam propagation direction implies angular momentum conservation. Along with the angular momentum selection rules, this limits the possible polarizations of the generated signal-idler photon pairs to $|LR\rangle$ and $|RL\rangle$. Since the process is coherent and $|LR\rangle$ and $|RL\rangle$ are indistinguishable otherwise, the resulting state $|\psi\rangle$ of a target mode photon pair can be written as

$$|\psi\rangle = a_0|LR\rangle + \exp(i\phi_0)\, a_1|RL\rangle\,. \tag{1}$$

The probability amplitudes $a_{0,1}$ and the phase ϕ_0 can be derived using a model based on the relative transition strength between different Zeeman sublevels [20, 21] as

$$a_{0,1} = \frac{x_{\alpha_S,\alpha_I}}{\sqrt{\sum\limits_{\alpha_S,\alpha_I=\pm 1}(x_{\alpha_S,\alpha_I})^2}}\,, \tag{2}$$

where $\alpha_{S,I}$ are the helicities of the signal and idler photons, and x_{α_S,α_I} is the product of relevant Clebsch-Gordan coefficients [24] that couple the individual $|m_F\rangle$ states of the different hyperfine levels involved in the four-wave mixing process, and

$$x_{\alpha_S,\alpha_I} = \sum_{m_F=-F_g}^{F_g} C^{F_g,1,F_b}_{m_F,-1,m_F-1}\, C^{F_b,1,F_e}_{m_F-1,1,m_F}\, C^{F_d,1,F_e}_{m_F-\alpha_S,\alpha_S,m_F}\, C^{F_g,1,F_d}_{m_F,-\alpha_I,m_F-\alpha_I}\,, \tag{3}$$

where $F_{g,b,e,d} = 2,2,3,3$ corresponding to the respective total angular momentum F of the participating levels. From (2), we obtain the expected state $|\psi_X\rangle \approx 0.55|LR\rangle - 0.83|RL\rangle$ for the decay path X. The reconstructed state ρ_X matches the expected one with a fidelity of 94±1%. For the decay path Y, the model predicts state $|\psi_Y\rangle \approx 0.92|LR\rangle - 0.39|RL\rangle$, which agrees with ρ_Y with a fidelity of 93±1%.

5. Transition strength of different decay paths

Both decay paths exhibit different decay time constants due to different transition strengths for the decays. The transition $5P_{3/2}, F = 3$ to $5S_{1/2}, F = 2$ is 2.8 times
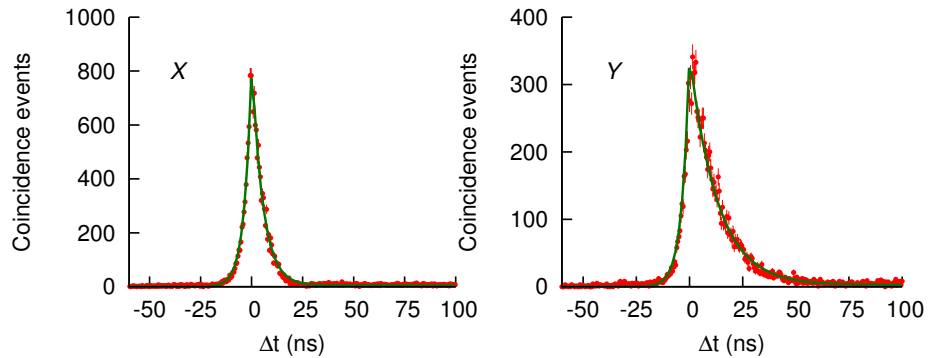
Figure 3. Coincidence events as a function of the detection time difference Δt between signal and idler photon detection for the decay path X and Y, selected with a temperature tuned etalon. Integration times were 7 and 14 minutes, respectively.

stronger than from $5P_{3/2}$, $F = 2$ [25]. This results in a higher optical density (OD) for the $F = 3$ transition [26], and should lead to a faster decay via path X [27]. To experimentally investigate this, we perform separate time correlation measurements between the detection of signal and idler photons for each decay path. The histogram of coincidence events as a function of time delay Δt between the detection of signal and idler photons sampled into 1 ns wide time bins is shown in figure 3. The solid line in both cases shows a fit to a heuristic model, inspired by the joint effect of a decay time corresponding to the two-photon transition [15, 28], and the effect of a finite ring-down time of the filter etalon:

$$G_{X,Y}^{(2)}(\Delta t) = \begin{cases} G_0 \, \exp(\Delta t/\tau_r) & \text{for } \Delta t < 0 \\ G_0 \, \exp(-\Delta t/\tau_{X,Y}) & \text{for } \Delta t \geq 0 \, . \end{cases} \quad (4)$$

For path X, we obtain a decay constant $\tau_X{=}5.6{\pm}0.1$ ns for an idler photon heralded by a signal photon. In the same way, with the etalon tuned to transmit the resonance frequency of the $5P_{3/2}$, $F = 2 \rightarrow 5D_{3/2}$, $F = 3$ transition for path Y, we find $\tau_Y{=}$ $13.1{\pm}0.2$ ns. Both decay constants $\tau_{X,Y}$ are shorter than the spontaneous decay time $\tau_{sp} = 27$ ns of the $5P_{3/2}$ level of a single Rubidium atom in free space due to the collective enhancement effects observed in an optically thick atomic ensemble .

The rise time $\tau_r = 3.1 \pm 0.3$ ns for decay path X and $\tau_r = 3.3 \pm 0.4$ ns for Y is a consequence of the finite response time of the etalon. Both values are compatible with the value of 3.0 ± 0.1 ns obtained in an independent characterization of the etalon.

6. Quantum beats

Without the etalon (see figure 1), the decay paths X and Y cannot be distinguished by wideband photodetectors. Consequently, the energy difference between photons from the two paths leads to a modulation of the time correlation function between signal
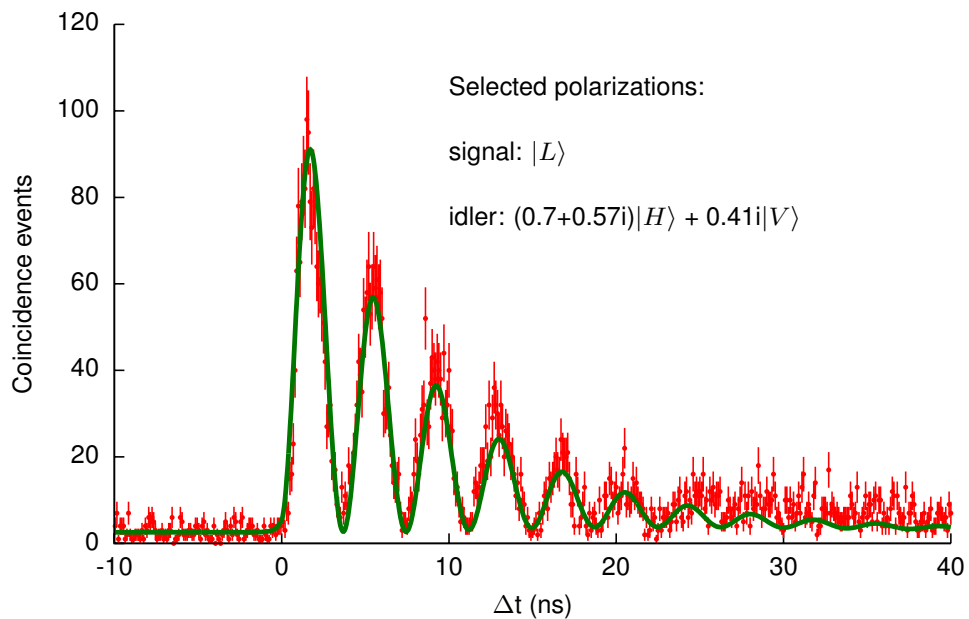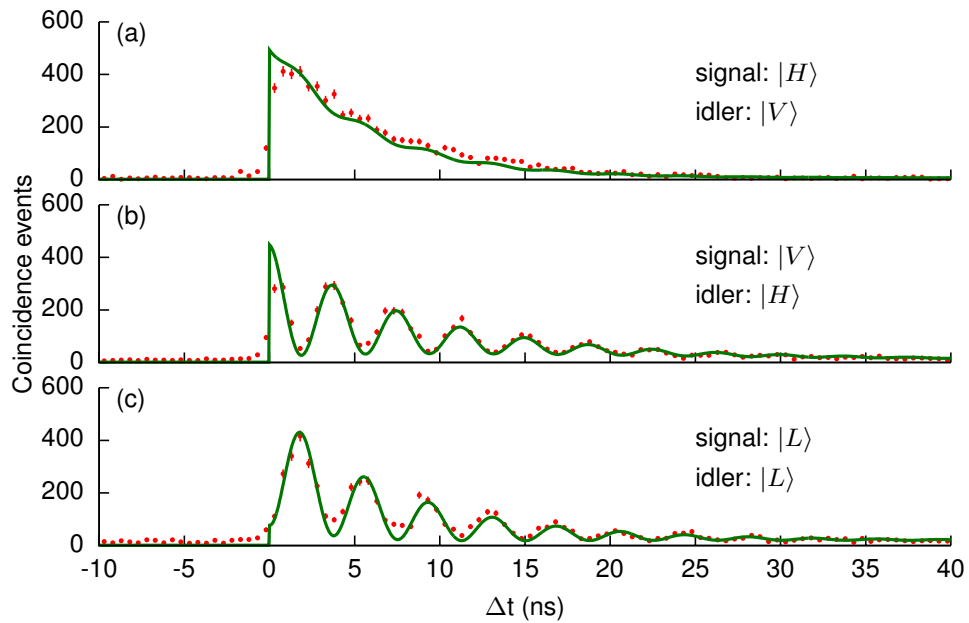
Figure 4.   Coincidences as a function of the time delay between the detection of signal and idler photons, with no etalon in the signal mode. Pump 1 and 2 are set to orthogonal linear polarization H and V, respectively, and signal and idler are projected onto the polarization states $|L\rangle$ and $(0.7 + 0.57i)|H\rangle + 0.41i\,|V\rangle$. The observed modulation ("quantum beat") is associated with the hyperfine splitting of $266\,\text{MHz}$ between $F = 3$ and $F = 2$ of the $5P_{3/2}$ level. To resolve the oscillations with high contrast, avalanche photodetectors with a low time jitter ($\approx 40\,\text{ps}$) were used for this measurement. Due to the lower quantum efficiency of these detectors, the total acquisition time is 5 hours.

and idler photodetection, as shown in Figure 4. This, and other similar phenomena, is known as quantum beats: it was predicted at an early stage of quantum physics [29], and first experimentally observed in pulsed optical excitation of atoms with two upper states decaying to the same ground state [30, 31]. Quantum beats have also been observed in cascade decay systems of dilute atomic vapours [32], dense thermal atomic vapours [33], and for single ions [34].

In our case, the beat frequency $\delta/2\pi{=}266\,\text{MHz}$ is equal to the energy difference between the hyperfine levels $5P_{3/2}$, $F = 3$ and $F = 2$. The measurements shown in Figure 4 are performed with polarization of pump 1 and 2 set to H and V, respectively, and polarizations of signal and idler modes are set to observe a large interference contrast.

To model the interference between the different decay paths, we take into account the different coherence time of the emitted photon pairs, characterized by the time constants τ_X and τ_Y, and the relative difference in the generation amplitude R, and phase ϕ. These last two terms can be calculated via (2). We express the probability amplitudes $c_{X,Y}$ for paths X and Y as function of the detection time difference Δt

Figure 5. Coincidence rate as a function of time delay between the detection of signal and idler photons for different choices of polarization of signal and idler photons. (a) The beats are damped by choosing the appropriate polarizations due to suppression of coincidences from decay path Y. $R = 2.86 * 10^{-2}$ and $\phi = \pi$, total acquisition time 9 minutes. (b) and (c): different polarization projections change the phase of the oscillation. In this two cases, the relative phase difference is π. (b) $R = 1.43$ and $\phi = 0$, total acquisition time 35 minutes; (c) $R = 0.5$ and $\phi = \pi$, total acquisition time 28 minutes.

between signal and idler photons,

$$c_X(\Delta t) = \Theta(\Delta t) G_0 \, e^{-\frac{\Delta t}{2\tau_X} - i\omega_i \Delta t}, \quad \text{and} \quad c_Y(\Delta t) = \Theta(\Delta t) G_0 R \, e^{-\frac{\Delta t}{2\tau_Y} - i(\omega_i + \delta)\Delta t + \phi}, \quad (5)$$

which interfere to a joint detection probability

$$\begin{aligned} G^{(2)}(\Delta t) &= |c_X + c_Y|^2 \\ &= \Theta(\Delta t) G_0^2 \left[e^{-\frac{\Delta t}{\tau_X}} + R^2 e^{-\frac{\Delta t}{\tau_Y}} + 2R \, e^{-\frac{\Delta t(\tau_X + \tau_Y)}{2(\tau_X \tau_Y)}} \cos\left(\delta \, \Delta t + \phi\right) \right] (6) \end{aligned}$$

Using the measured coherence times τ_X and τ_Y and the values of R and ϕ calculated from the interaction strengths of the transitions, we fit the experimental data in figure 4 using (6) with only G_0 and an accidental count rate as free parameters, and find a good agreement with this relatively simple model.

Different interaction strengths for the different polarizations in the participating levels allow control of the relative amplitude and phase of the possible decay paths. We can observe the dependence of the amplitude of the oscillation on the polarization settings and compare it with the expected values calculated from the interaction strengths of the transitions. In figure 5 we present three different cases, all fitted in a similar way as for figure 4. Of particular interest is the case where the beats are

almost entirely suppressed [figure 5(a)], an indication that most of the photon pairs observed are generated by the X decay. Figure 5(b) and (c) show the situation for polarization selections that lead to quantum beats with a high contrast, but opposite phases.

This demonstrates that it is possible to select one frequency component only by an appropriate choice of polarizations, without using an etalon. However, it is not possible to select only photon pairs from the Y decay in a similar manner due to the relative weakness of the transitions involving the $5P_{3/2}$, $F = 2$ level.

7. Conclusion

In summary, we have characterized the polarization entangled state of photon pairs from a cold cloud of atoms by performing quantum state tomography, individually for two decay paths of the cascade. We find that the resulting polarization-entangled states for both decay paths are not maximally entangled, but reasonably close to it. This is compatible with a model combining the transition strengths between different participating intermediate states in the four-wave mixing process. We observe high-contrast quantum beats in a time correlation measurement between the generated photon pairs. The contrast and the initial phase of beats can be controlled with the choice of polarization of pumps and projective measurements on the generated photons.

Acknowledgments

[1] Brunner N, Cavalcanti D, Pironio S, Scarani V and Wehner S 2014 *Rev. Mod. Phys.* **86**(2) 419–478 URL http://link.aps.org/doi/10.1103/RevModPhys.86.419
[2] Nielsen M A and Chuang I L 2004 *Quantum Computation and Quantum Information* 1st ed (Cambridge University Press) ISBN 0521635039
[3] Fry E S 1973 *Phys. Rev. A* 1219
[4] Aspect A, Grangier P and Roger G 1982 *Phys. Rev. Lett.* **49**(2) 91–94
[5] Fiorentino M, Voss P L, Sharping J E and Kumar P 2002 *Photonics Technology Letters, IEEE* **14** 983–985
[6] Kuzmich A, Bowen W P, Boozer A D, Boca A, Chou C W, Duan L M and Kimble H J 2003 *Nature* **423** 731–734
[7] Balić, Vlatko, Braje, Danielle A, Kolchin, Pavel, Yin, G Y and Harris, Stephen E 2005 *Phys. Rev. Lett.* **94** 183601
[8] Chanelière T, Matsukevich D N, Jenkins S D, Kennedy T A B, Chapman M S and Kuzmich A 2006 *Phys. Rev. Lett.* **96**(9) 093604
[9] Gisin N, Ribordy G, Tittel W and Zbinden H 2002 *Rev. Mod. Phys.* **74**(1) 145–195 URL http://link.aps.org/doi/10.1103/RevModPhys.74.145
[10] Englert B G, Kurtsiefer C and Weinfurter H 2001 *Phys. Rev. A* **63**(3) 032303 URL http://link.aps.org/doi/10.1103/PhysRevA.63.032303
[11] Aspect A, Grangier P and Roger G 1981 *Phys. Rev. Lett.* **47**(7) 460–463
[12] Kwiat P G, Mattle K, Weinfurter H, Zeilinger A, Sergienko A V and Shih Y 1995 *Phys. Rev. Lett.* **75**(24) 4337–4341 URL http://link.aps.org/doi/10.1103/PhysRevLett.75.4337

[13] Willis R T, Becerra F E, Orozco L A and Rolston S L 2011 *Opt. Express* **19** 14632–14641
[14] Muller M, Bounouar S, Jons K D, Glassl M and Michler P 2014 *Nat Photon* **8** 224–228 URL http://dx.doi.org/10.1038/nphoton.2013.377
[15] Srivathsan B, Gulati G K, Chng B, Maslennikov G, Matsukevich D and Kurtsiefer C 2013 *Phys. Rev. Lett.* **111** 123602
[16] Gulati G K, Srivathsan B, Chng B, Cerè A, Matsukevich D and Kurtsiefer C 2014 *Phys. Rev. A* **90**(3) 033819 URL http://link.aps.org/doi/10.1103/PhysRevA.90.033819
[17] James D F V, Kwiat P G, Munro W J and White A G 2001 *Phys. Rev. A* **64**(5) 052312
[18] Coffman V, Kundu J and Wootters W K 2000 *Phys. Rev. A* **61**(5) 052306
[19] Wootters W K 1998 *Phys. Rev. Lett.* **80**(10) 2245–2248
[20] Jenkins S D, N D, Chanelière T, Lan S Y, Kennedy T A B and Kuzmich A 2007 *J. Opt. Soc. Am. B* **24** 316–323
[21] Jenkins S D 2006 *Theory of Light Atomic Ensemble Interactions: Entanglement, Storage, and Retrieval* Ph.D. thesis Georgia Institute of Technology
[22] Boyd R W 2008 Chapter 1 - the nonlinear optical susceptibility *Nonlinear Optics (Third Edition)* ed Boyd R W (Burlington: Academic Press) pp 1 – 67 third edition ed ISBN 978-0-12-369470-6
[23] Matsukevich D N, Chanelière T, Bhattacharya M, Lan S Y, Jenkins S D, Kennedy T A B and Kuzmich A 2005 *Phys. Rev. Lett.* **95**(4) 040405 URL http://link.aps.org/doi/10.1103/PhysRevLett.95.040405
[24] Metcalf H and van der Straten P 1999 *Laser Cooling and Trapping* Graduate Texts in Contemporary Physics (Springer New York) ISBN 9780387987286
[25] Steck D 2001 Rubidium 87 d line data URL http://steck.us/alkalidata/
[26] Foot C J 2005 *Atomic Physics* Oxford Master Series in Atomic, Optical and Laser Physics (OUP Oxford) ISBN 0198506961
[27] Jen H H 2012 *Phys. Rev. A* **85** 013835 URL http://link.aps.org/doi/10.1103/PhysRevA.85.013835
[28] Jen H H 2012 *J. Phys. B: At. Mol. Opt. Phys.* **45** 165504
[29] Breit G 1933 *Rev. Mod. Phys.* **5**(2) 91–140 URL http://link.aps.org/doi/10.1103/RevModPhys.5.91
[30] Aleksandrov E 1964 *Optics and Spectroscopy* **17** 522
[31] Dodd J N, Sandle W J and Zissermann D 1967 *Proceedings of the Physical Society* **92** 497
[32] Aspect A, Dalibard J, Grangier P and Roger G 1984 *Opt. Commun.* **49**(6) 429
[33] Bacerra F, Willis R, Rolston S and Orozco L 2011 *Revista Mexicana De Físca S* **57**(3) 23–28
[34] Schug M, Kurz C, Eich P, Huwer J, Müller P and Eschner J 2014 *Phys. Rev. A* **90**(2) 023829